

# Effects of Chip Load on Phase Transformation and Residual Stress in Silicon Grinding

Yung-Yuan Liao\*, Jiunn-Jyh Junz Wang\*\* and Chao-Yu Huang\*\*\*

**Keywords :** Silicon grinding, chip load, plowing, phase transformation, residual stress

## ABSTRACT

This study examines the surface formation mechanism, near-surface residual stresses, phase transformations, and their interrelationships in surface grinding of silicon (100) under various chip loading conditions. Near-surface residual stresses of the ground surfaces are found to be all compressive for all chip loading conditions with the transverse residual stress more affected by the chip load. Through Raman spectra of the ground surface, it is shown that the Si-I phase tends to transform to Si-III/Si-XII at a larger chip load, and to amorphous phase at a smaller chip load. SEM surface topography reveals that the degree of plowing in surface formation increases with chip load, and that surface residual stress and phase transformation can be correlated to the extent of plowing phenomenon on the silicon surface during the material removal process. It is concluded that grinding condition with higher chip load leads to the formation of Si-III/Si-XII phases as well as a higher transverse surface residual stress while a smaller chip load is favorable in the formation of an amorphous phase and low residual stress.

## INTRODUCTION

Grinding plays an important role in the mechanical processing of semiconductor and optical materials such as silicon, germanium and sapphire etc.

*Paper Received December, 2018. Revised March, 2019. Accepted April, 2019. Author for Correspondence: Jiunn-Jyh Wang*

\* General Manager, CHAO-WEI Precision Co., LTD  
[theoliao@gmail.com](mailto:theoliao@gmail.com)

\*\* Professor, Department of Mechanical Engineering, National Cheng Kung University No. 1, Dasyue Rd., Tainan, Taiwan, 701.  
[jjwang@mail.ncku.edu.tw](mailto:jjwang@mail.ncku.edu.tw)

\*\*\* Chief, Instrument Calibration Section, Systems Sustainment Center, National Chung-Shan Institute of Science and Technology.  
[cyhuang@ncsist.org.tw](mailto:cyhuang@ncsist.org.tw)

However, high stress contact between the abrasives and silicon has been shown to induce near-surface phase changes and residual stress, both having negative effect on the performance of circuits fabricated on the affected silicon substrate (Nix, 1989; Bullis et al., 1999). A better understanding of the silicon behavior under high stress grinding condition is therefore crucial to the control of mechanical process-induced surface damage.

In its natural state, silicon exists in a diamond-like crystal structure (Si-I). Results from diamond anvil cell experiment, indentation and scratch tests, have shown silicon can transform to several forms when subjected to high pressure under room temperature (Gerk and Tabor, 1978; Domnich and Gogotsi, 2002). Under hydraulic loading condition, Si-I was shown to be transformed into the metallic  $\beta$ -tin structure (Si-II) at a high pressure of 11~12GPa (Wentorf and Kasper, 1963; Minomura and Drickmer, 1962). The resistance measurement has shown that the resistivity of silicon decreases rapidly by an order of 5 under a certain high pressure, indicating the formation of a metallic phase (Minomura and Drickmer, 1962; Clarke et al., 1988; Ruffell, 2007). However, this phase is not stable at ambient pressure. Upon unloading, the resistivity will increase to a value lower than or equal to the normal state. It was experimentally found that, depending on the unloading condition, Si-II can transform to various metastable phases. With slow unloading rate, there exists a transition from the Si-II structure to the metastable phase, the R8 or Si-XII (Kailer et al., 1997), which is named for its rhombohedra lattice with eight atoms in the basis. With further release at the same rate, R8 is shown to transform to the body centered cubic structure, BC8 (or Si-III), at about 2~6 GPa (Grain et al., 1994). Finally, a mixture of both phases remains at the ambient pressure. However, on rapid pressure release, transmission electron microscopy analyses have given evidences on the formation of an amorphous silicon phase (a-Si) (Yan et al., 2005; Daibin et al., 2003; Duclos et al., 1990; Puttick et al., 1994).

Since silicon interacting with the abrasives of a grinding wheel experiences similar loading/unloading process as in the scratch test, phase transformation and amorphization have also been observed in silicon

lapping and grinding processes. Through Raman spectra analysis, the silicon surface was shown to transform to a uniform layer of amorphous phase (a-Si) after a lapping process (Verkey, et al., 1994). Also through Raman spectra, various phases of Si-IV, Si-XII, Si-III and a-Si were found in chips from wafer dicing and a-Si was found on ground surface after lapping and edge grinding processes (Gogotsi et al., 1999). Residual stress was also detected by Raman shift on these surfaces. On polishing of silicon with #500 abrasives, a transformed a-Si layer of 30-80 nm was reported along with the existence of residual compressive stress of 150 MPa (Chen and Wolf, 2003). Yan (2008) investigated the ductile and brittle silicon removal mechanism in the rough and fine grinding processes and showed that an a-Si surface was formed in the fine grinding process. Although these studies have shown the existence of phase transformation and residual stress in silicon grinding; the effects of chip load on their formation and interrelationships among the chip load, surface formation mechanism, phase changes and residual stress have not yet been reported.

The objective of this study is to investigate the formations of surface, phase changes and residual stresses in surface grinding of silicon wafer under various chip loading conditions. The topography of ground surface is examined by scanning electron microscope to reveal the surface deformation mechanism. Micro Raman spectroscopy is used to investigate the phases induced in silicon. Magnitude and spread of the residual stresses is evaluated by the indentation technique. Finally, correlation between grinding-induced phase transformation and residual stress is discussed as related to the removal mechanism of silicon.

### MEASUREMENT OF RESIDUAL STRESS BY THE INDENTATION TECHNIQUE

In this study, the residual stress on ground surface is measured by the indentation technique (Johnson-Walls et al., 1986; Suresh and Giannakopoulos, 1998; Tandon, 2007; Gruninger et al., 1987; Kese and Rowcliffe, 2003; Kobrin and Harker, 1989). A developed crack system under Vickers test for silicon without and with residual stress is illustrated in Figure 1, showing smaller horizontal crack length in the x direction due to the presence of residual compression stress in the y direction. For the same Vickers' load, based on the analysis from Kese and Rowcliffe (2003), the residual stress,  $\sigma_r$ , can be shown to be

$$\sigma_r = \frac{K_c}{\psi c^{1/2}} \left[ 1 - \left( \frac{c_0}{c} \right)^{3/2} \right] \quad (1)$$

where  $K_c$  represents critical stress intensity factor,  $\psi$  is a constant related to the crack geometry and

loading conditions. Since the present problem can be simplified as a penny crack,  $\phi$  is set to be  $2/\pi^{1/2}$  (Lawn, 1993).  $c_0$  is the crack length in the absence of the residual stress, and  $c$  is the new equilibrium length. By measuring the indentation crack length without and with the residual stress, the magnitude of the residual stress can be directly calculated from Eq. (1).

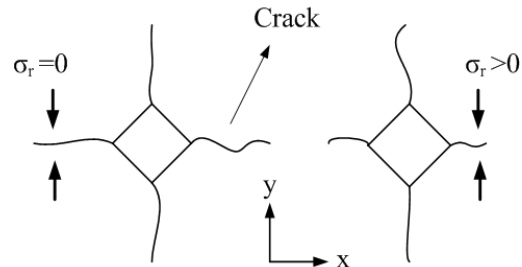


Figure 1. Effect of residual stress on the crack length of Vickers indentation, without residual stress (left) and with residual stress.

### EXPERIMENTAL SETUP

The experiments were carried out on a surface grinding machine using a resin bonded diamond grinding wheel. A commercial single crystal silicon wafer (100) of 0.63 mm in thickness was sawn into squares of 50 mm x 50 mm to be used as the work material, which is fixed on the machine by a vacuum chuck. Figure 2 illustrates the configuration of the grinding experiment. Dry cutting was performed without any cutting fluid to avoid any contamination or chemical effects. The resin bonded diamond wheels, D-1800-N-100-B, have an average grit size of 7  $\mu\text{m}$  with 25% volume ratio of diamond grit. The feed speed,  $f$ , was set to be 5 mm/s. The wheel cutting speed,  $V$ , was fixed at 31 m/s at a rotation speed of 3300 rpm. To see the effects of chip load on the silicon phases and residual stresses, three different wheel depths of cut of 2, 4 and 6  $\mu\text{m}$  are chosen, corresponding to the maximum uncut chip thickness of 20, 28, and 35 nm, respectively (Shaw, 1996).

Before each grinding experiment, the resin bonded diamond wheels are dressed by pre-grinding on a rotary alumina wheel to a cumulative depth removal of 0.5 mm at a linear grinding speed of 6 m/s. The surface of silicon workpiece is pre-conditioned with a continuous sequence of fine grinding process at a wheel depth of cut of 0.5  $\mu\text{m}$  to obtain a fine, smooth surface. This fine grinding sequence is similar to the spark-out process in steel grinding, where continuous back-forth grinding strokes are performed on a workpiece without resetting the wheel depth until the spark vanishes.

For each depth of cut, grinding experiment is carried out on four silicon workpieces. For each workpiece, the following data are acquired: three SEM images, Raman spectra from four spots and residual stress at four separate locations. Raman

spectra on the ground surface were detected by a micro Raman spectrometer (Renishaw 2000) with a spectral resolution of  $1 \text{ cm}^{-1}$ . An argon laser (514.5 nm) of 17 mW was used as the light source. A 63X objective lens was used to form a  $1 \mu\text{m}$  laser spot size on the sample. The spot size and power were selected to optimize the signal while minimizing laser-beam heating effect. As for the measurement of the residual stresses on the ground surface, the fracture characteristics of indentation test were observed by an optical microscope to determine the crack length in the longitudinal and transverse directions. In this study, both up and down grinding have been conducted, but without any noted difference in the resulting phase changes and residual stresses. Therefore, only results from down grinding are presented.

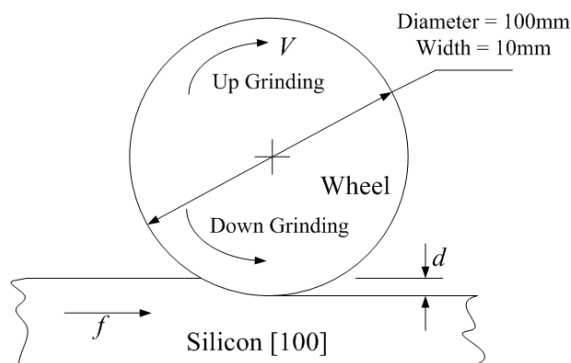


Figure 2. Schematic illustration of the surface grinding process.  $V=31 \text{ m/s}$ ,  $f=5 \text{ mm/s}$ ,  $d=2-6 \mu\text{m}$ .

## RESULTS AND DISCUSSIONS

### Effects of Chip load on Surface Topography of Ground Silicon

The pre-conditioning process for silicon squares before each experiment is a fine-grinding process with a very light chip load. Shown by the SEM images in figure 3(a), the surface of pre-conditioned silicon workpiece is characterized by plastically deformed silicon, an evidence of ductile cutting. This ductile fracture is expected since the uncut chip thickness in the pre-conditioning process, starting at a maximum of 10nm for the first stroke, are smaller than the silicon's critical depth of cut of 30 nm for a ductile to brittle fracture transition (Bifano et al., 1991). As the wheel depth of cut increases, the chip load increases, leading to change in the material removal mechanism and different surface topography. Typical SEM images of ground surface at depths of cut of 2, 4 and 6  $\mu\text{m}$  are shown in figure 3(b, c, d). As chip load increases with larger depth of cut, signs of plowing mark with pile-up and grooved ridges are more evident on the surface. Although ductile deformation is still the prevalent material removal and surface formation mechanism

for all depths of cut, signs of brittle fracture such as cavities and cracks become more apparent at wheel depth of cut of 6  $\mu\text{m}$ , figure 4(d), as the maximum uncut chip thickness of some abrasives has exceeded the critical depth of cut for ductile deformation due to a natural spread in the random chip load distribution of a grinding process (Hecker et al., 2007).

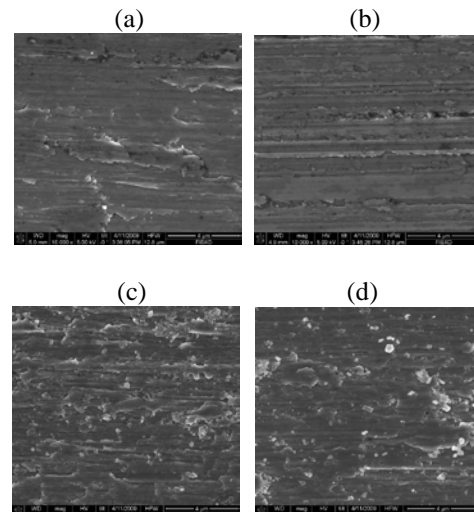


Figure 3. SEM image of ground silicon surface (10000X) for down grinding at different wheel depth of cut for (a) pre-conditioned, (b) 2  $\mu\text{m}$ , (c) 4  $\mu\text{m}$  and (d) 6  $\mu\text{m}$ . Grinding direction is from left to right.

### Effects of Chip Load on Near-Surface Residual Stresses

The residual stresses on each ground surface were evaluated using Eq. (1) by measuring the crack length of a 5 N Vickers indentation test. Figure 4 shows the magnitude and spread of residual stress in perpendicular and parallel to the grinding direction. These measurements indicate that residual stress varies significantly with the depth of cut as well as with the direction. Residual stresses in both the longitudinal and transverse directions for the three chip loads are all compressive. This result agrees with findings from Chen and Wolf (2003) and Immelmann et al. (1997) in the grinding of brittle materials. Furthermore, magnitude of transverse residual stresses at larger chip load is comparable to that found by Chen and Wolf (2003).

The residual stresses in both directions for the case of 2  $\mu\text{m}$  depth of cut are about the same at around -50 MPa level. At both 4  $\mu\text{m}$  and 6  $\mu\text{m}$  depths of cut, compressive residual stresses increase to  $-155 \pm 71 \text{ MPa}$  in the transverse direction, but only a slight compressive residual stress of about  $-10 \pm 8 \text{ MPa}$  is detected in the longitudinal direction.

The longitudinal residual stress is shown to be relatively independent of the chip loads at various depth of cut. The transverse residual stress is about

the same as the longitudinal one for small chip load, but becomes much greater at larger chip load. Correlation between the surface topography (figure 3) and the resulting residual stresses (figure 4) on ground silicon surface at various chip loads can provide an explanation on the effects of chip load on the degree of plowing and residual stress. Higher chip load results in higher contact stress and higher degree of plowing, and squeezing of silicon to the transverse direction. The squeezed silicon piles up to form ridges of the grinding groove in a way similar to the indentation test where the material flows and rises to the periphery of the impression. As in an indentation test, this plowing action of the grinding process will increase the compressive surface residual stress, which tends to close advancing crack induced by the indentation test along the grinding direction. The higher spread of residual stress in figure 4 can be explained by the larger variation of chip load and chip thickness associated with a larger wheel depth of cut as in Hecker et al. (2007).

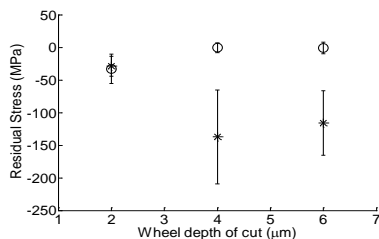


Figure 4. The surface residual stresses at three wheel depths of cut for down grinding.  $\ominus$ : longitudinal direction ;  $\star$ : transverse direction. Error bars show spread of measured data over 30 measurements.

### Effect of Chip Load on Process-induced Phase Transformation

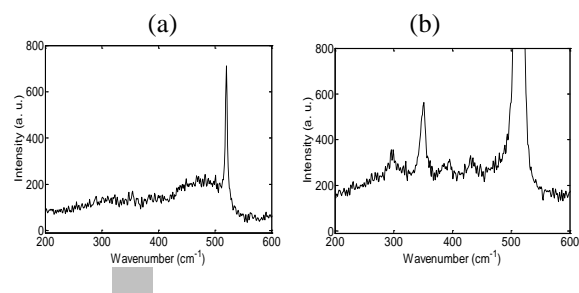
To observe the existence of process-induced phase transformation on preconditioned surface and ground surfaces under different chip loads, micro Raman spectroscopy was employed and four different types of spectrum are found to exist as shown in figure 5. Figure 5(a) shows a strong presence of amorphous silicon (a-Si), which has a broad band around  $470\text{ cm}^{-1}$ . The second type in Fig. 5(b) shows a strong presence of Si-III (BC8) and Si-XII (R8). Since the R8 or Si-XII structure is a rhombohedra distortion of BC8 or Si-III (Piltz et al., 1995), the two phases are expected to have similar pattern in Raman spectra. Raman bands at  $382$  and  $433\text{ cm}^{-1}$  can be attributed to the existence of Si-III, and the bands at  $350$  and  $394\text{ cm}^{-1}$  are major bands of Si-XII (Domnich and Gogotsi, 2002). This spectrum also shows a mixture of the two phases, R8/BC8 and a-Si. The third type shown in Fig. 5(c) has a similar Raman spectra to the second type only with less presence of Raman bands of R8/BC8 and is regarded as the transitional stage in this study. The last type of

spectrum shown in figure 5(d) is taken from brittle fracture region and only Si-I phase is present as indicated by a single Raman band at  $520\text{ cm}^{-1}$  corresponding to the bulk Si-I.

All of the Raman spectrum taken from preconditioned surfaces clearly indicates the presence of a-Si and Si-I, as shown in figure 5(a). This is similar to the result reported by Yan (2008), which showed that only an a-Si surface was formed in the fine grinding process. Figure 6 shows a histogram of detection count for the presence of various silicon phases on the ground surfaces, illustrating the influences of wheel depth of cut. It is shown that Si-III/Si-XII has a stronger presence at larger cutting depths of  $4\text{ }\mu\text{m}$  and  $6\text{ }\mu\text{m}$ , while amorphous phase is more dominant at the grinding depth of  $2\text{ }\mu\text{m}$ . Difference in the level of presence for each phase for each ground surface might be due to the combined effects of residual stresses and surface formation mechanism.

Both the metastable crystalline and amorphous silicon phase are found to exist under various chip loading conditions. By examining ground surface topography in figure 3 and phase changes in figure 6, surface with Si-III/Si-XII formation shows higher degree of plowing phenomenon than those of the amorphous phase. The amorphous phase can therefore be associated with light cutting and light plowing actions of the abrasives, as also reported by Clarke et al. (1998). At larger wheel depth of cut, larger chip load resistance leads to higher cutting and plowing actions, inducing transformation to metastable phases (Si-III/Si-XII).

Chip loading condition and depth of cut are generally known to affect the surface topography. Through this investigation, it is shown that chip loading condition not only affects the surface formation mechanism, but also has significant effects on the phase transformation and formation of residual stress on the ground silicon surface. These findings should help in the selection of chip loading condition for a better control of surface properties in the silicon grinding process. However, grinding is a complex process involving the selection of many more parameters, including type, size, volume and bonding of abrasives, work and wheel speeds, etc. More researches are therefore needed for further understandings of the silicon material responses in a general grinding process.



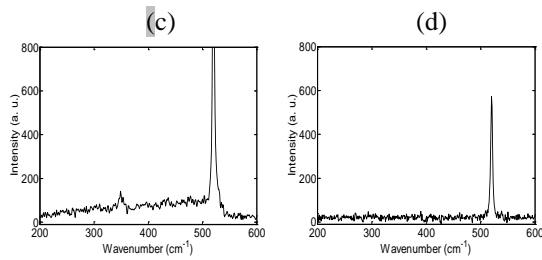


Figure 5. Four types of the Raman spectra taken from ground silicon surface. (a) amorphous silicon (a-Si) around 470  $\text{cm}^{-1}$ , (b) Si-XII around 350  $\text{cm}^{-1}$ , 394  $\text{cm}^{-1}$  and Si-III around 382  $\text{cm}^{-1}$ , 433  $\text{cm}^{-1}$ , (c) transitional stage, (d) Si-I

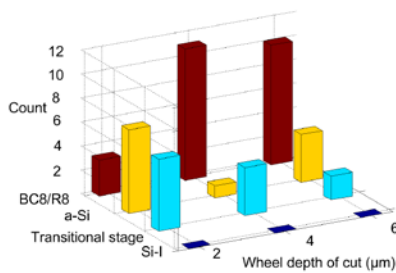


Figure 6. The event count for various phases at different wheel depth of cut for down grinding. Each experiment included 17 measured data.

## CONCLUSIONS

This paper aims to achieve a better understanding of the silicon behavior under various chip loading conditions in the surface grinding of silicon. Experiments have been carried out to investigate the effects of chip load on plowing phenomenon, near-surface residual stress and phase transformation, and to reveal their interrelationships. The following conclusions can be drawn from this investigation:

- (1) Near-surface residual stresses on the ground surfaces are found to be all compressive for all chip loading conditions. For smaller chip load at wheel depth of cut of 2  $\mu\text{m}$ , residual stresses in both transverse and longitudinal directions are both small and about the same. The transverse residual stress increases at higher chip load while the longitudinal residual stress remains small for all chip loading conditions.
- (2) Through Raman spectra of the ground surface, it is shown that the bulk Si-I phase tends to transform to Si-III/Si-XII at a larger chip load, and amorphous phase tends to occur at a smaller chip load.
- (3) At various chip loads, correlation of SEM surface topography and phase changes reveals that surface with Si-III/Si-XII formation shows higher degree of plowing phenomenon than those of the amorphous phase.

- (4) The interrelationship among plowing phenomenon in surface formation, residual stress and phase changes in silicon is presented. Grinding condition with higher chip load leads to higher plowing action, the formation of Si-III/Si-XII phases as well as a higher transverse surface residual stress while a smaller chip load is favorable in the formation of an amorphous phase accompanied by lower residual stresses.

## ACKNOWLEDGEMENTS

This work was partially supported by the “Intelligent Manufacturing Research Center” (iMRC) from The Featured Areas Research Center Program within the framework of the Higher Education Sprout Project by the Ministry of Education (MOE) in Taiwan.

## REFERENCES

- Bifano, T.G., Dow, T.A. and Scattergood, R.O. “Ductile-Regime Grinding: a New Technology for Machining Brittle Materials,” *ASME Journal of Engineering for Industry.*, Vol.113, pp.184–189 (1991).
- Bullis, W.M., Lin, W., Wagner, P., Abe, T. and Kobayashi, S., Defects in silicon (III), Seattle, WA, *The Electrochemical Society* (1999).
- Chen, J. and Wolf, I.D., “Study of damage and stress induced by backgrinding in Si wafers,” *Semiconductor Science and Technology.*, Vol.18, pp.261-268 (2003).
- Clarke, D.R., Kroll, M.C., Kirchner, P.D., Cook, R.F. and Hockey, B.J., “Amorphization and conductivity of silicon and germanium induced by indentation,” *Physical Review Letters.*, Vol.60, pp.2156–2159 (1988).
- Clarke, D.R., Kroll, M.C., Kirchner, P.D., Cook, R.F. and Kockey, B.J., “Amorphization and conductivity of silicon and germanium induced by indentation,” *Physical Review Letters.*, Vol.60, pp.2156–2159 (1998).
- Crain, J., Ackland, G.J., Maclean, J.R., Piltz, R.O., Hatton, P.D. and Pawley, G.S., “Reversible pressure-induced structure transitions between metastable phases of silicon,” *Physical Review B.*, Vol.50, pp.13043 – 13046 (1994).
- Daibin, G., Dommich, V. and Gogotsi, Y., “High-resolution transmission electron microscopy study of metastable silicon phases produced by nanoindentation,” *Journal of Applied Physics.*, Vol.93, pp.2418 – 2423 (2003).
- Dommich, V. and Gogotsi, Y., “Phase transformation in silicon under contact loading,” *Rev. Adv.*

- Mater. Sci.*, 3 1–36 (2002).
- Duclos, S.J., Vohra, Y.K. and Ruoff, A.L., “Experimental study of crystal stability and equation of state of Si to 248Gpa,” *Physical Review B.*, Vol.41, pp.12021–12028 (1990).
- Gerk, A.P. and Tabor, D., “Indentation hardness and semiconductor-metal transition of germanium and silicon,” *Nature.*, Vol.271, pp.732–733, (1978).
- Gogotsi, Y., Baek C. and Kirscht, F., “Raman microspectroscopy study of processing-induced phase transformations and residual stress in silicon,” *Semiconductor Science and Technology.*, Vol.14, pp.936-944 (1999).
- Gruninger, M.F., Lawn, B.R., Farbaugh, E.N. and Wachtman, J.B. JR., “Measurement of residual stresses in coatings on brittle substrates by indentation fracture,” *Journal of the American Ceramic Society.*, Vol.70, pp.344–48 (1987).
- Hecker, R.L., Liang, S.Y., Wu, X.J., Xia, P. and Jin, D.G.W., “Grinding force and power modeling based on chip thickness analysis,” *The International Journal of Advanced Manufacturing Technology.*, Vol.33, pp.449–459 (2007).
- Immelmann, S., Welle, E. and Reimers, W., “X-ray residual stress analysis on machined and tempered HPSN-ceramics,” *Materials Science and Engineering A.*, Vol.238, pp.287–292 (1997).
- Johnson-Walls, D., Evans, A.G., Marshall, D.B. and James, M.R., “Residual stresses in machined ceramic surface,” *Journal of the American Ceramic Society.*, Vol.69, pp.44–47 (1986).
- Kailer, A., Gogotsi, Y.G. and Nickel, K.G., “Phase transformations of silicon caused by contact loading,” *Journal of Applied Physics.*, Vol.81, pp.3057–3063 (1997).
- Kese, K. and Rowcliffe, D.J., “Nanoindentation method for measuring residual stress in brittle materials,” *Journal of the American Ceramic Society.*, Vol.86, pp.811–816 (2003).
- Kobrin, P. H. and Harker, A. B., “The effects of thin compressive films on indentation fracture toughness measurements,” *Journal of Materials Science.*, Vol.24, pp.1363–1367 (1989).
- Lawn, B.R., “Fracture of brittle solids,” Cambridge University Press Cambridge (1993).
- Minomura, S. and Drickamer, H.G., “Pressure induced phase transitions in silicon, germanium and some III-V compounds,” *Journal of Phys. Chem. Solids.*, Vol.23, pp.451–456 (1962).
- Nix, W.D., “Mechanical properties of thin films,” *Metallurgical Transactions A.*, Vol.20A, pp.2217–2245 (1989).
- Piltz, R.O., Maclean, J.R., Clark, S.J., Ackland, G.J., Hatton, P.D. and Crain, J., “Structure and properties of silicon XII: a complex tetrahedrally bonded phase,” *Physical Review B.*, Vol.52, pp.4072–4085 (1995).
- Puttick, K. E., Whitmore, L.C., Chao, C.L. and Gee, A. E., “Transmission electron microscopy of nanomachined silicon crystals,” *Philosophical Magazine A.*, Vol.69, pp.91-103 (1994).
- Ruffell, S., Bradby, J.E., Fujisawa, N. and Williams, J.S., “Identification of indentation-induced changes in silicon by in situ electrical characterization,” *Journal of Applied Physics.*, Vol.101, pp.083531-1–083531-7 (2007).
- Shaw, M.C., “Principles of Abrasive Processing,” Oxford University Press New York (1996).
- Suresh, S. and Giannakopoulos, A.E., “A new method for estimating residual stresses by instrumented sharp indentation,” *Acta Materialia.*, Vol.46, pp.5755–5767 (1998).
- Tandon, R. “A technique for measuring stresses in small spatial regions using cube-corner indentation: application to tempered glass plates,” *Journal of the European Ceramic Society.*, Vol.27, pp.2407–2414 (2007).
- Verhey, J., Bismayer, U., Guttler, B. and Lundt, H., “The surface of machined silicon wafers: a Raman spectroscopic study,” *Semiconductor Science and Technology.*, Vol.9, pp.404-408 (1994).
- Wentorf, R.H. and Kasper, J.S., “Two new forms of silicon,” *Science.*, Vol.139, pp.338–339 (1963).
- Yan, J., Takahashi, H., Tamaki, J., Gai, X. and Kuiyagawa, T., “Transmission electron microscopy observation of indentations made on ductile-machined silicon wafer,” *Applied Physics Letters.*, Vol.87, pp.211901-1–211901-3 (2005).
- Yan, J., “Process induced subsurface damage in mechanically Ground Silicon Wafers,” *Semiconductor Science and Technology.*, Vol.23, 075038 (10pp) (2008).

## 切屑負載對矽研磨加工中 相變化和殘留應力影響之 研究

廖永源 王俊志 黃朝鈺  
國立成功大學機械工程學系

## 摘要

本研究探討不同切屑負載下矽(100)表面研磨中表面形成機制、近表面殘留應力、相變化及其相互關係。發現在所有切屑負載條件下，近表面殘留應力皆為壓應力，而縱向殘留應力受切屑負載影響較大。通過表面的拉曼光譜，可見Si-I相在較大的切屑負載下趨於轉變為Si-III / Si-XII，而在較小的切屑負載下趨於轉變為非晶相。SEM表面形貌顯示在材料去除過程中，隨著切屑負載增加，表面生成之犁切現象增加，並直接影響表面殘留應力和相變化。實驗結果發現，切屑負載較高的磨削條件會導致形成Si-III / Si-XII相以及較高的橫向殘餘應力，而較小的切屑載荷則有利於形成非晶相和較低的殘留應力。